Journal of Thermal Analysis and Calorimetry, Vol. 80 (2005) 625–629

THERMAL CHARACTERIZATION OF CHEMICALLY REDUCED ELECTROLYTIC MANGANESE DIOXIDE

B. Liu[1], *P. S. Thomas*[1*], *R. P. Williams*[2] *and S. W. Donne*[3]

[1]Department of Chemistry, Materials and Forensic Sciences, University of Technology, Sydney, PO Box 123, Broadway, NSW 2007, Australia
[2]Delta-EMD Australia Pty Limited, McIntosh Drive, Mayfield West, 2304, Australia
[3]Discipline of Chemistry, University of Newcastle, Callaghan, NSW 2308, Australia

Samples of electrolytic manganese dioxide (EMD) were chemically reduced using 2-propanol under reflux (82°C) for 1, 2, 3, 6 and 24 h intervals. XRD analysis showed that the γ-MnO_2 structure was preserved although the lattice dimensions were observed to increase with increasing degree of reduction to accommodate the intercalation of protons. The exception was the 24 h reduced sample which contained two phases; γ-MnO_2 and γ-MnOOH. Three regions of decomposition in the range of 50 to 1000°C were observed using thermogravimetric analysis coupled with mass spectrometry (TG-MS) and were accounted for as water removal below 390°C, reduction of MnO_2 to Mn_2O_3 between 400 and 600°C, and Mn_2O_3 to Mn_3O_4 between 600 and 1000°C. Again the exception proved to be the 24 h reduced sample which was observed to decompose predominantly in one step between 400 and 600°C directly to Mn_3O_4.

Keywords:*electrolytic manganese dioxide, reduction, TG-MS, X-ray crystallography*

Introduction

The current alkaline dry cell battery market is dominated by the use of electrolytic manganese dioxide (EMD) as the cathode material [1]. EMD is produced by anodic electrolytic deposition from solution producing a complex morphology (for example; the crystallite size and distribution, porosity and surface area) due to the non-equilibrium nature of the deposition process in an electrochemical cell. The structure is of the γ-MnO_2 form, which results from lattice faults produced during deposition, and is essentially a blend or intergrowth of pyrolusite (β-MnO_2) and ramsdellite domains. As the deposition process is electrochemical precipitation from solution, water is also an integral part of the structure and influences the electrochemical performance in application. Characterisation of EMD morphology and its relation to performance as a cathode material is, therefore, of technological importance.

Of the techniques that have been applied to the characterisation of manganese dioxides, thermal analysis has provided some insight into the character of the water as well as the mechanisms of thermal decomposition. For a typical thermogravimetric characterisation of manganese dioxide, water is first observed to be evolved. Three types of water, designated I, II and III, have been reported [2, 3]. Type I water is regarded as being strongly bound physisorbed molecular water and is removed around 100°C; the removal of Type II water around 200°C is irreversible and is related to the removal of surface bound hydroxyl groups and water of crystallisation; and the removal of Type III water around 300°C is related to the removal of the bulk of hydroxyl groups. The character of the water contained in the EMD is important as it impacts on the performance of the material in application as the mechanism of charge transfer is based on the intercalation of protons into the γ-MnO_2 structure as the EMD is reduced [1, 4]:

$$MnOOH_r+\Delta H_2O+\Delta e^- \rightarrow MnOOH_{r+\Delta}+\Delta OH^- \quad (1)$$

where *r* represents the level of proton insertion [1, 4].

Upon heating beyond the water loss stage, decomposition of the MnO_2 occurs which results in the reduction of manganese(IV) to manganese(II) oxide (MnO); MnO being the final product produced on heating to 1500°C [5]. The reduction process occurs through a series of decomposition steps of lower oxide stoichiometries [5, 6]:

$$MnO_2 \xrightarrow{I} Mn_2O_3 \xrightarrow{II} Mn_3O_4 \xrightarrow{III} MnO \quad (2)$$

The actual mechanism for the thermal reduction of manganese oxides is known to be a function of the origin and history of the specimen as well as the environment in which the reduction is carried out [5–11]. Indeed, for EMD some of these steps, in particular Step I in Eq. (2), have been shown to be a complex series of reduction processes through intermediate stoichiometric

* Author for correspondence: paul.thomas@uts.edu.au

1388–6150/$20.00

Akadémiai Kiadó, Budapest, Hungary
Springer, Dordrecht, The Netherlands

compositions [6]. In order to improve the understanding of the complex thermo-chemistry of manganese oxides, in particular EMD, this paper furthers the investigation of the effect of structure, processing history and origin on the decomposition mechanism by characterising the thermal decomposition of a range of partially chemically reduced specimens of EMD using thermogravimetric analysis coupled with evolved gas analysis (TG/EGA) as well as X-ray crystallography for the identification of the phases present.

Experimental

EMD was supplied by Delta EMD Australia Pty Limited and was determined to be γ-MnO_2 by X-ray diffraction (XRD) analysis. 10 g samples of the EMD specimen was chemically reduced under reflux (82°C) in 50 mL of AR grade 2-propanol. The reduction reactions were stopped at 1, 2, 3, 6 and 24 h. The reduced EMD specimens were recovered by filtration and thoroughly washed with acetone. The specimens were then vacuum dried and stored in a desiccator.

The determination of x in MnO_x, i.e. the degree of reduction, was carried out based on the potentiometric titration method described by Vetter and Jaeger [12]. The partially reduced EMD specimens prepared were examined by TG/EGA using a Setaram Setsys 16/18 thermobalance coupled with a Balzers ThermoStar mass spectrometer for evolved gas analysis. All experiments were carried out in an alumina (Al_2O_3) crucible at a heating rate of 5 K min^{-1} from ambient temperature to 1200°C under flowing (20 mL min^{-1}) high purity argon gas. XRD experiments were carried out on Siemens D5000 X-ray diffractometer with CuK_α radiation from 15 to 100° 2θ at 0.02° 2θ s^{-1}. X-ray analysis was also used to identify structural changes in different regions of the TG/DTG curves. Specimens were heat-treated to the various plateaus of the TG curves, cooled and characterized using XRD.

Results and discussion

The degree of reduction *vs*. reflux time of chemically reduced EMD specimens is shown in Fig. 1. As expected the value of x in MnO_x is observed to decrease with increasing reduction time. XRD patterns of each reflux reduced specimen are shown in Fig. 2 with the position of the (221)/(240) peak around 55° 2θ plotted as a function of reduction time in Fig. 1. The peak shift to lower value of 2θ represents an increase in the lattice dimensions through the inclusion of protons in the structure as reduction proceeds. The specimens of up to three hours reflux reduction time have retained their

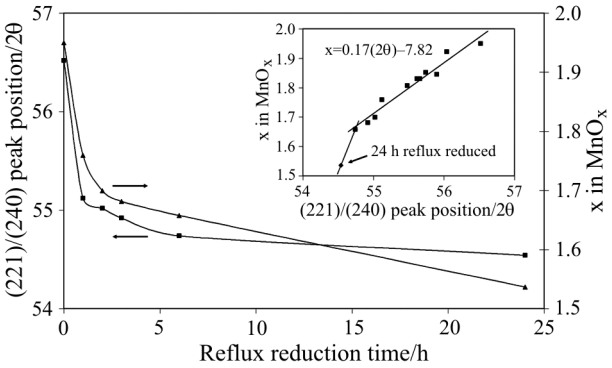

Fig. 1 Degree of reduction of EMD as measured by x in MnO_x plotted as a function of time and as a function of the position of the (221)/(240) XRD peak. The inset is a plot of x in MnO_x as a function of the position of the (221)/(240) XRD peak. Included in this plot is data for room temperature reduced (up to 24 h) specimens of EMD. Error in the value of x in MnO_x determined from the linear fit (not including the 24 h reflux reduced specimen) is estimated to be 6%

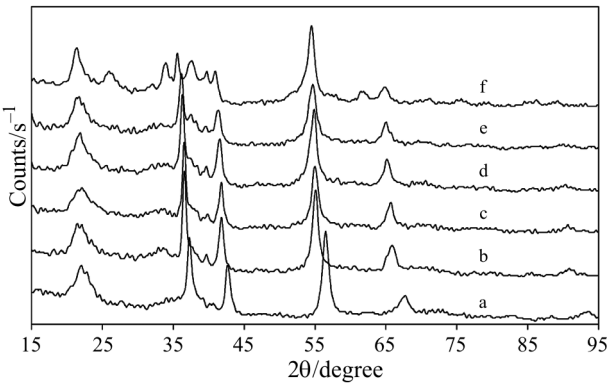

Fig. 2 XRD patterns of reflux reduced EMD: a – as received, b – 1 h, c – 2 h, d – 3 h, e – 6 h, f – 24 h

γ-MnO_2 structure indicating incorporation of protons in the lattice. Similarly, the predominant structure evident for the 6 h specimen is that of γ-MnO_2 with only trace amounts of γ-MnOOH observed. The structure of the 24 h reflux reduced specimen is observed to be a mix of γ-MnO_2 and γ-MnOOH and contains significant proportions of the γ-MnOOH. The effect of reduction on the XRD data is also observed in the inset in Fig. 1 where value of x in MnO_x is observed to be approximately a linear function of the position of the 55° 2θ peak (excluding the 24 h reflux reduced specimen). The outlying point in this plot is the 24 h reduced peak thus also indicating a change in phase morphology. It should be noted that, in addition to the reflux reduced specimen data, specimens reduced at room temperature in isopropanol for up to 24 h are also included.

TG and DTG data for each specimen are shown in Figs 3 and 4. Three regions of decomposition were

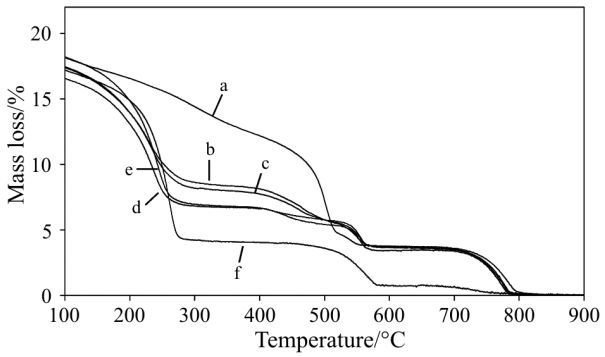

Fig. 3 TG curves of: a – as received, b – 1 h, c – 2 h, d – 3 h, e – 6 h, f – 24 h reflux reduced EMD. Note: The mass loss has been normalised to the sample mass at 1000°C where it is in the final product form, Mn_3O_4, which all samples produce. This gives a better indication of the mass of bound water in the reduced EMD specimens. The 24 h curve also shows Mn_2O_3 to Mn_3O_4 transformation which is not observed in the XRD analysis

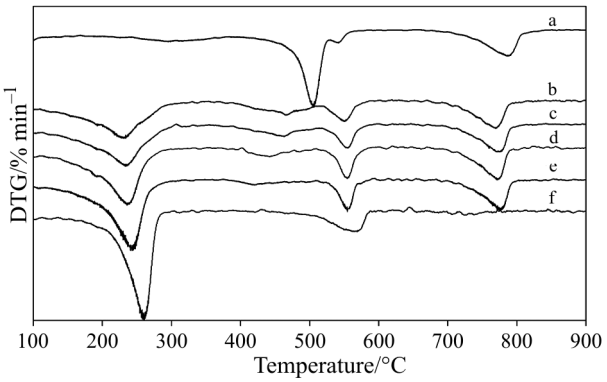

Fig. 4 DTG curves of: a – as received, b – 1 h, c – 2 h, d – 3 h, e – 6 h, f – 24 h reflux reduced EMD

observed based on three general steps in each of the TG curves. The temperature ranges of these regions are: Region 1 – room temperature to 390°C, Region 2 – 390 to 610°C and Region 3 – 610 to 1200°C. Mass loss data for these regions are shown in Table 1.

Region 1 is observed to be comprised mainly of the removal of water from each specimen, namely physisorbed molecular water and structural water i.e. water of crystallisation and chemically bound water (Fig. 5). This is also confirmed by XRD data of the 3 h reflux reduction sample heat-treated at 310°C (Fig. 6) where the structure remains characteristic of γ-MnO_2 indicating that mass loss in this region is entirely due to water loss from the specimen. Water removal from the unreduced specimen occurred throughout the region indicating a range of energetic states in which the water is bound. The three types of water (Type I, II and III) at temperatures 100, 200 and 300°C reported by Lee *et al*. [2] are not easily identified in the TG/DTG data (Figs 3 and 4). A peak is observed centred on 310°C correlating with the Type III water. Further deconvolution of the water types is aided by the MS data where two overlapping peaks are observed and centred at approximately 227 and 290°C accounting for Type II and III water (Fig. 5). Type I (physisorbed) water is also present as mass is also observed to be lost in the low temperature part of this region.

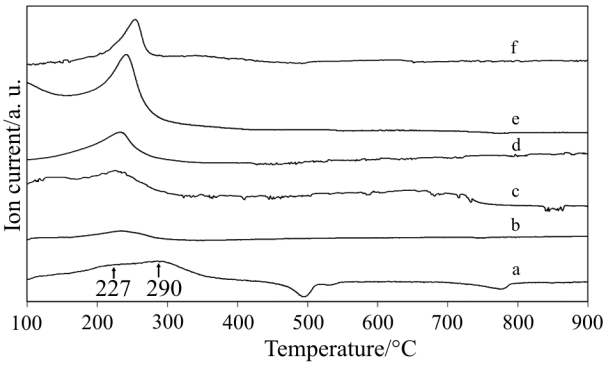

Fig. 5 MS curves of water ion fragment measured at 18 amu: a – as received, b – 1 h, c – 2 h, d – 3 h, e – 6 h, f – 24 h reflux reduced EMD

The effect of chemical reduction is most simply observed in the increasing degree of mass loss in this region with increasing degree of reduction (Table 1). The degree of reduction is also observed to have an effect on the peak temperature of the water loss peak. For each of the reduced specimens a single peak dominates the region with increasing degree of reduction shifting the peak to higher temperature. The water loss peak

Table 1 Mass loss (%) for different regions corresponding to peaks in the DTG data (Fig. 4)

Sample	x in MnO_x	Region 1 water loss peak	Region 2 oxygen loss peak 1	Region 2 oxygen loss peak 2	Region 3 oxygen loss peak
unreduced	1.95	3.5	6.5	0.6	3.1
1 h	1.76	8.0	2.3	1.6	3.0
2 h	1.70	8.2	2.0	1.6	3.0
3 h	1.68	8.4	1.1	1.7	2.9
6 h	1.66	10.3	0.93	1.7	3.0
24 h	1.54	11.3	–	2.7	0.5

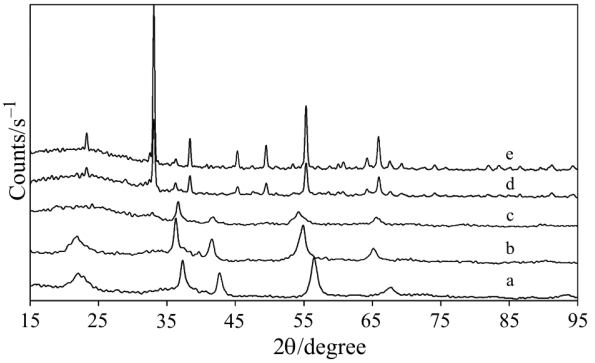

Fig. 6 XRD patterns of heat-treated 3 h reflux reduced EMD: a – as received, b – no heat treatment, c – 310°C, d – 500°C, e – 600°C

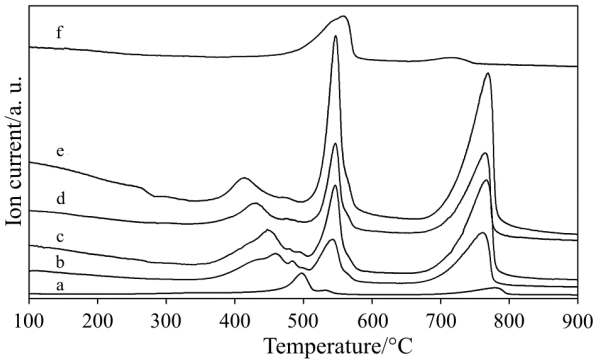

Fig. 8 MS curves of oxygen ion fragment measured at 32 amu: a – as received, b – 1 h, c – 2 h, d – 3 h, e – 6 h, f – 24 h reflux reduced EMD

also becomes sharper suggesting a greater concentration of bound water with the same energetics indicating that the protons are being incorporated in the lattice in a more ordered manner.

Although in this region only water is lost from the 24 h reduced sample, from the XRD data obtained for a sample heat-treated to 310°C (Fig. 7), the specimen is observed to be a mixture of α-Mn_3O_4 and Mn_5O_8. Given the presence of these two species, it is likely that the removal of water has resulted in the disproportionation of the MnOOH present [13]:

$$8MnOOH \rightarrow Mn_3O_4 + Mn_5O_8 + 4H_2O \quad (3)$$

The MS curve for oxygen evolution (Fig. 8) shows no trace of oxygen evolution below 400°C. The lack of oxygen evolution also suggests disproportionation as only water was observed to be removed.

Region 2 (390 to 610°C) corresponds to the first of the manganese reduction steps, MnO_2 to Mn_2O_3, resulting in the evolution of oxygen:

$$2MnO_2 \rightarrow Mn_2O_3 + 1/2O_2 \quad (4)$$

Evidence for the reduction stoichiometry of Eq. (4) is found in the XRD data in Fig. 6 where the oxide species observed at 600°C, with the exception of the 24 h specimen, is Mn_2O_3. The decomposition mechanism, however, is observed to be more complex with at least two steps involved in the reduction. The 'as received' EMD shows two peaks in this region at 506 and 540°C corresponding to a two-step decomposition process [6]:

$$7MnO_2 \rightarrow Mn_5O_8 + Mn_2O_3 + 3/2O_2 \quad (5)$$

$$2Mn_5O_8 \rightarrow 5Mn_2O_3 + 1/2O_2 \quad (6)$$

For the reduced specimens, this region also comprises of two decomposition peaks at around 460 (shifting to lower temperature with increasing reduction) and 556°C. The dominant peak in the 'as received' specimen is the lower temperature peak at 506°C. For the reduced specimens, the dominant step is the higher temperature step. Only a single peak at 560°C is observed for the specimen reduced for 24 h.

For the 3 h reduced sample, evidence of Mn_5O_8 is apparent in the 2θ=28° peak observed in curve d in Fig. 6 suggesting that Eqs (5) and (6) represent at least part of the reaction sequence for the reduced specimens. The predominant phase observed in curve d is, however, Mn_2O_3. It is likely that this is due to the fact that, as time is taken to cool the specimen from 500°C to room temperature, further reaction would have occurred resulting in partial completion of the second step. The oxygen data shown in Fig. 8 indicate that the first step is quite complex with at least 3 peaks observed in the data below 500°C (with the exception of the 24 h reduced specimen). Equations (5) and (6) can, therefore, only be indicative of the reduction process observed in the partially reduced specimens. The lower temperature peak observed in the DTG (Fig. 4) and the EGA data (Fig. 8) also shifts to lower temperature from 460°C in the 1 h specimen to 420°C in the 6 h reduced specimen. This decline suggests that the γ-MnO_2 structure has become increasingly strained as intercalated protons fill an increasing proportion of the available lattice interstices with increasing degree of reduction.

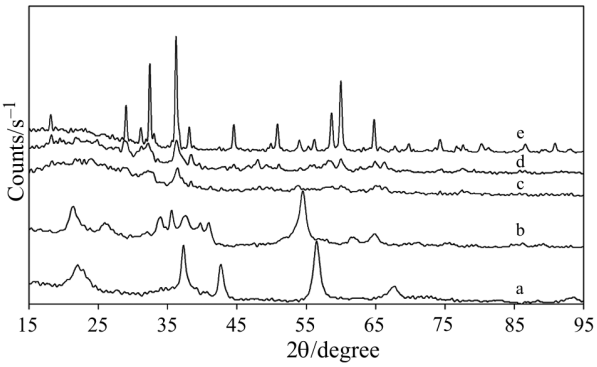

Fig. 7 XRD patterns of heat-treated 24 h reflux reduced EMD: a – as received, b – no heat treatment, c – 310°C, d – 430°C, e – 600°C

XRD analysis of the 430°C pattern of the 24 h reduced specimen (curve d in Fig. 7) indicates the presence of both Mn_5O_8 and Mn_3O_4. At 600°C only Mn_3O_4 is observed. The peak at 560°C is, therefore, likely to correspond to the decomposition of Mn_5O_8 to Mn_3O_4 as has been reported elsewhere for the thermal decomposition of γ-MnOOH [13]:

$$3Mn_5O_8 \rightarrow 5Mn_3O_4 + 2O_2 \quad (7)$$

Region 3 is in the temperature range of 670 to 870°C and is characterised by the decomposition of Mn_2O_3 to Mn_3O_4 resulting in the reduction of the manganese and loss of oxygen from the specimen [6, 13]:

$$6Mn_2O_3 \rightarrow 4Mn_3O_4 + O_2 \quad (8)$$

This peak is observed for all specimens around 780°C. The peak is also present in the 24 h reflux reduced specimen, but the magnitude is very small (0.5% in mass loss) in comparison and is likely to be associated with the decomposition of small proportions of unreduced EMD in the original specimen; although the source of this mass loss does require further investigation.

The effect of reflux reduction has been observed in changes to the lattice dimensions, changes in phase morphology and changes in the decomposition mechanism. For a degree of reduction up to x in MnO_x of 1.68 (3 h reflux), the effect on the lattice is apparently limited to the expansion of the lattice dimensions as indicated by a reduction in the values of 2θ for the diffraction peaks. For the 6 h (x=1.66) reduced species the presence of MnOOH was identified, however, the predominant structure remained in keeping with incorporation of protons in the γ-MnO_2 lattice (Figs 1 (inset) and 2). MnOOH was observed in significant proportions in the 24 h reduced specimen (x=1.54). From XRD analysis 'saturation' of the γ-MnO_2 lattice is, therefore, apparent at a value of x in the region of 1.66 below which (i.e. if further reduction is allowed to occur) phase transformation occurs to form the γ-MnOOH structure. This is also reflected in the thermal analysis data where significant differences in the decomposition mechanism for the 24 h reflux reduced specimen were observed. The actual transition point is, however, difficult to define as the thermal analysis of the 6 h reduced specimen suggests a decomposition mechanism more in keeping with the shorter time reduction samples.

Conclusions

TG and XRD characterisation of EMD has confirmed that EMD has a significant capacity for reduction without significant change to the overall structure through the intercalation of protons in the γ-MnO_2 lattice. The γ-MnO_2 structure was observed to be retained up to significant degrees of reduction (to a value of x in MnO_x of approximately 1.66). For x<1.66 a second phase, γ-MnOOH, was observed to be formed. The change in the phase morphology resulted in a change in the mechanism of thermal decomposition. EGA analysis proved to be extremely sensitive to the decomposition process. This was particularly true of the oxygen ion (32 amu) data where multiple peaks were observed indicating a complex decomposition process in the 390 to 600ºC region for partially reduced specimens. Further investigation is, however, required to elucidate the origins of these multiple steps and to relate these findings to evaluation of EMD performance in application.

References

1 S. Donne, R. Fredlein, G. Lawrance, D. Swinkels and F. L. Tye, Prog. Batteries Battery Mater., 13 (1994) 113.
2 J. A. Lee, C. E. Newnham and F. L. Tye, J. Colloid Interface Sci., 42 (1973) 372.
3 J. A. Lee, C. E. Newnham and F. L. Tye, J. Chem. Soc., Faraday Trans., 74 (1978) 237.
4 J. Fitzpatrick and F. L. Tye, J. Appl. Electrochem., 21 (1991) 130.
5 B. D. Desai, J. B. Fernandes and V. N. K. Dalal, J. Power Sources, 16 (1985) 1.
6 B. Liu, P. S. Thomas, A. S. Ray and R. P. Williams, J. Therm. Anal. Cal., 76 (2004) 115.
7 P. R. Skidmore, Prog. Batteries Sol. Cells, 9 (1990) 167.
8 M. I. Zaki, M. A. Hasan, L. Pasupulety and K. Kumari, Thermochim. Acta, 302 (1997) 171.
9 R. Giovanoli, Prog. Batteries Battery Mater., 13 (1994) 50.
10 C. Gonzalez, J. I. Gutierrez, J. R. Gonzalez-Velasco, A. Cid, A. Arranz and J. F. Arranz, J. Therm. Anal. Cal., 52 (1998) 985.
11 G. A. El-Shobaky, A. M. Ghozza and H. A. Hassan, J. Therm. Anal. Cal., 51 (1998) 529.
12 N. Jaeger and K. J. Vetter, Electrochim. Acta, 11 (1966) 401.
13 A. Agopsowicz, J. L. Hitchcock and F. L. Tye, Thermochim. Acta, 32 (1979) 63.